

## LETTERS

# Voltage-dependent electrogenic chloride/proton exchange by endosomal CLC proteins

Olaf Scheel<sup>1\*</sup>, Anselm A. Zdebik<sup>1\*</sup>, Stéphane Lourdel<sup>1</sup> & Thomas J. Jentsch<sup>1</sup>

Eukaryotic members of the CLC gene family function as plasma membrane chloride channels, or may provide neutralizing anion currents for V-type H<sup>+</sup>-ATPases that acidify compartments of the endosomal/lysosomal pathway<sup>1</sup>. Loss-of-function mutations in the endosomal protein CLC-5 impair renal endocytosis<sup>2</sup> and lead to kidney stones<sup>3</sup>, whereas loss of function of the endosomal/lysosomal protein CLC-7 entails osteopetrosis<sup>4</sup> and lysosomal storage disease<sup>5</sup>. Vesicular CLCs have been thought to be Cl<sup>-</sup> channels, in particular because CLC-4 and CLC-5 mediate plasma membrane Cl<sup>-</sup> currents upon heterologous expression<sup>6,7</sup>. Here we show that these two mainly endosomal CLC proteins instead function as electrogenic Cl<sup>-</sup>/H<sup>+</sup> exchangers (also called antiporters), resembling the transport activity of the bacterial protein CLC-e1 (ref. 8), the crystal structure of which has already been determined<sup>9</sup>. Neutralization of a critical glutamate residue not only abolished the steep voltage-dependence of transport<sup>7</sup>, but also eliminated the coupling of anion flux to proton counter-transport. CLC-4 and CLC-5 may still compensate the charge accumulation by endosomal proton pumps, but are expected to couple directly vesicular pH gradients to Cl<sup>-</sup> gradients.

To investigate whether CLC-4 or CLC-5 display Cl<sup>-</sup>/H<sup>+</sup> exchange activity, as observed for the *Escherichia coli* protein CLC-e1 (ref. 8), we measured the intracellular pH of transfected tsA201 cells using the pH-dependent fluorescence of 2',7'-bis-(2-carboxyethyl)-5-(and-6)-carboxyfluorescein (BCECF). In apparent contrast to such an exchange activity, intracellular pH did not change when lowering the extracellular Cl<sup>-</sup> concentration ([Cl<sup>-</sup>]<sub>o</sub>). However, currents of CLC-4 and CLC-5 were only detected at positive intracellular voltages<sup>6,7</sup>. If these currents reflect electrogenic Cl<sup>-</sup>/H<sup>+</sup> exchange, H<sup>+</sup> transport may only be observed upon depolarization. Intracellular pH was therefore recorded in response to changes of the plasma membrane voltage. The plasma membrane was patch-clamped and exposed to different voltages using the gramicidin-perforated patch technique that prevented the loss of BCECF and limited the exchange of protons with the patch pipette. If there was an electrogenic exchange of Cl<sup>-</sup> for H<sup>+</sup>, then depolarizing the membrane should lead to an efflux of H<sup>+</sup>; that is, to a cytosolic alkalization. Indeed, exposure of patch-clamped cells transfected with CLC-4 or CLC-5 to positive voltages resulted in an increase of intracellular pH (Fig. 1a–c). No significant change in intracellular pH was detected when imposing negative voltages (Fig. 1a). The voltage dependence of the rate of intracellular pH change ( $\Delta pH_i/\Delta t$ ; Fig. 1e, f) correlated well with the steep voltage dependence of CLC-4 or CLC-5 currents<sup>6,7</sup> (Fig. 2a). Depolarization of cells changes the driving force for H<sup>+</sup> and may cause alkalization in the presence of an H<sup>+</sup> conductance; however, non-transfected cells lacked significant changes to intracellular pH in response to depolarization. Furthermore, depolarizing cells expressing a Cl<sup>-</sup> conductance will increase intracellular Cl<sup>-</sup> concentration ([Cl<sup>-</sup>]<sub>i</sub>), which might, in turn, cause an alkalization of the cytoplasm

through endogenous Cl<sup>-</sup>/HCO<sub>3</sub><sup>-</sup> (or Cl<sup>-</sup>/OH<sup>-</sup>) exchangers. However, control cells expressing the *Torpedo* Cl<sup>-</sup> channel CLC-0 did not alkalize upon depolarization, although their Cl<sup>-</sup> currents were of similar magnitude (Fig. 1d).

Hence, the depolarization-induced alkalization of cells expressing CLC-4 or CLC-5 was neither due to a changed driving force for H<sup>+</sup>, nor to an intracellular accumulation of chloride. Strong evidence for Cl<sup>-</sup>/H<sup>+</sup> exchange came from experiments in which H<sup>+</sup> was driven against its electrochemical gradient (Fig. 1c). Cells expressing CLC-4 or CLC-5 were exposed to an extracellular pH of 5.0, creating a chemical H<sup>+</sup> gradient of 120 mV (assuming an intracellular pH of 7.0), from which the depolarization to +60 mV must be subtracted to obtain the electrochemical gradient for H<sup>+</sup>. Hence, the resulting cytoplasmic alkalization (Fig. 1c) demonstrated H<sup>+</sup> transport against an electrochemical gradient of more than 60 mV.

In the bacterial CLC-e1 protein, the coupling of chloride flux to protons was abolished when a critical glutamate was mutated to alanine (E148A)<sup>8</sup>. In the CLC-e1 crystal, the negative side chain of this glutamate blocks the access of extracellular anions to the narrowest part of the pore<sup>9</sup>. The equivalent mutations E224A and E211A in CLC-4 and CLC-5, respectively, converted their currents from being strongly outwardly rectifying to having a nearly ohmic behaviour<sup>7</sup>, as shown for CLC-5 in Fig. 2a, b. Whereas extracellular acidification reduced the currents of wild-type CLC-4 and CLC-5 proteins<sup>7</sup>, the anion conductance of the respective glutamate mutants was independent of extracellular pH (Fig. 2a–c). This suggests that these mutations, similar to CLC-e1 (ref. 8), eliminate the H<sup>+</sup> coupling of anion currents. Indeed, depolarizing cells expressing these mutants failed to induce alkalization (Fig. 2d).

If CLC-4 and CLC-5 are Cl<sup>-</sup>/H<sup>+</sup> exchangers, changes in extracellular anion concentrations should affect the counter-transport of H<sup>+</sup>. To depolarize cells to voltages compatible with the transport activity of CLC-4 or CLC-5, they were co-transfected with the peptide-gated snail Na<sup>+</sup> channel FaNaC<sup>10,11</sup> (Fig. 3). Patch-clamp experiments revealed that its ligand H-Phe-Met-Arg-Phe-NH<sub>2</sub> (FMRFamide) depolarized the cells to roughly +30 mV. Exposure of cells co-expressing CLC-5 and FaNaC to FMRFamide induced alkalization with 150 mM, but not with 4 mM, extracellular Cl<sup>-</sup> (Fig. 3a). Such effects were not seen when FaNaC was expressed alone or together with the CLC-5 E211A mutant. The alkalization observed upon exposure to FMRFamide and 150 mM Cl<sup>-</sup> could be reversed by lowering [Cl<sup>-</sup>]<sub>o</sub> to 4 mM (Fig. 3b), just opposite to pH changes expected with anion exchangers. This intracellular pH recovery was absent when cells were hyperpolarized by Na<sup>+</sup> removal to inhibit Cl<sup>-</sup>/H<sup>+</sup> exchange (Fig. 3c), suggesting that Cl<sup>-</sup>/H<sup>+</sup> exchange mediates the pH recovery.

The observed decrease of currents upon extracellular acidification<sup>7</sup> (Fig. 2a, c) is compatible with the notion that currents directly reflect an electrogenic Cl<sup>-</sup>/H<sup>+</sup> exchange, because increasing [H<sup>+</sup>]<sub>o</sub> would

<sup>1</sup>Zentrum für Molekulare Neurobiologie, ZMNH, Universität Hamburg, Falkenried 94, D-20246 Hamburg, Germany.

\*These authors contributed equally to this work.

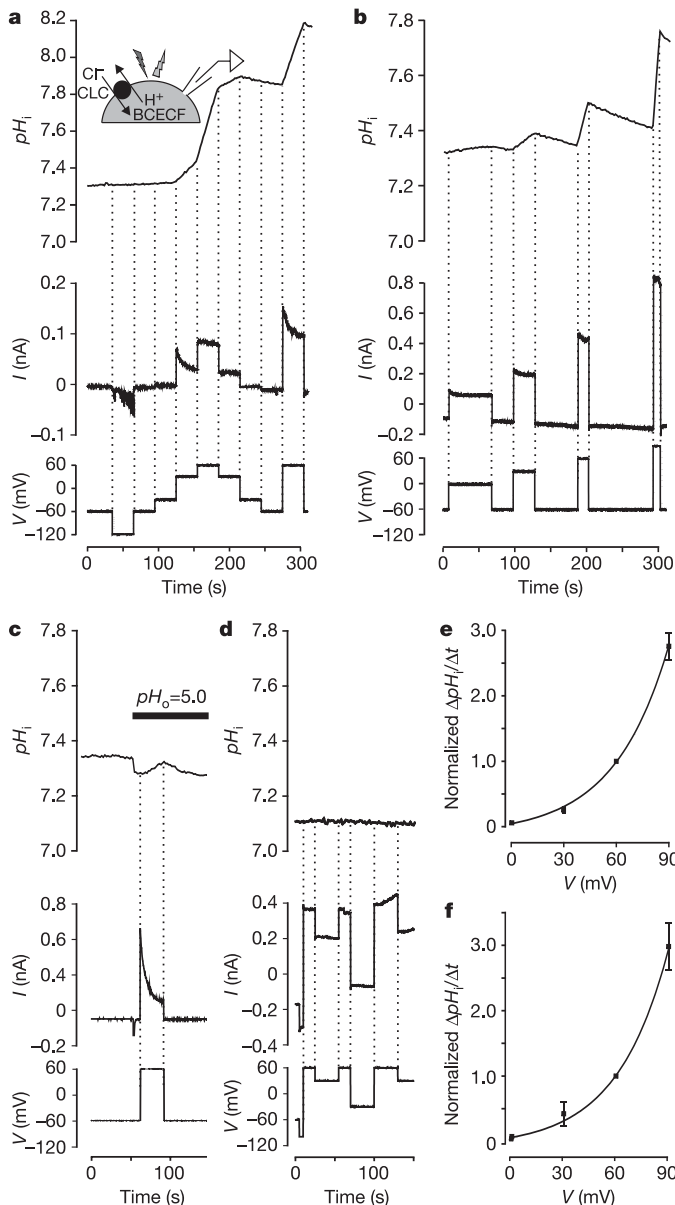


**Figure 1 | Depolarization alkalinizes cells expressing CIC-4 or CIC-5, but not those expressing CIC-0.** **a–d**, Measurements of intracellular pH ( $pH_i$ ; top panel), clamp current (middle panel) and clamp voltage (bottom panel) of tsA201 cells transfected with CIC-4 (**a**, **c**), CIC-5 (**b**), or CIC-0 (**d**). Cells were voltage clamped using gramicidin-perforated patches, and intracellular pH was determined using BCECF fluorescence (inset in **a**). Current relaxations with depolarizing pulses may reflect a rise in  $[Cl^-]_i$ . Similar results were obtained with 6, 13 and 7 cells for CIC-4, CIC-5 and CIC-0, respectively. **c**, Depolarization alkalinizes a CIC-4-transfected cell also with an extracellular pH ( $pH_o$ ) of 5.0, demonstrating  $H^+$  transport against its electrochemical gradient. Similar results were obtained with 5 and 9 cells for CIC-4 and CIC-5, respectively. Intracellular pH also dropped upon extracellular acidification in untransfected controls. The acidification upon returning to  $-60$  mV (**a–c**) probably represents pH equilibration over the patch. **e**, **f**, Rates of intracellular pH change as a function of clamp voltage for CIC-4 (**e**) and CIC-5 (**f**). Results were obtained using protocols as in **b**, and represent means from 5 and 8 cells for CIC-4 and CIC-5, respectively. Data were normalized to  $\Delta pH_i/\Delta t$  at 60 mV. Error bars indicate s.e.m.

lower the gradient driving the exchanger. Unfortunately, the extreme outward rectification of currents mediated by CIC-3, CIC-4 and CIC-5 precludes a reliable determination of reversal potentials that could be used to calculate the coupling ratio, as done for the bacterial protein CIC-e1 (ref. 8). We therefore estimated the stoichiometry of

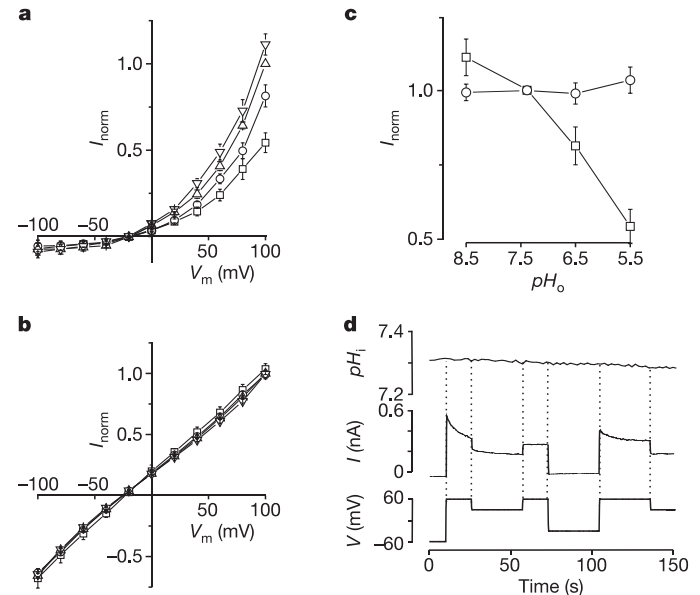


**Figure 2 | The E211A mutation abolishes flux coupling to  $H^+$ .** **a**, **b**, Steady-state  $I$ - $V$  for CIC-5 (**a**) and CIC-5(E211A) (**b**) expressed in *Xenopus* oocytes. Extracellular pH was varied between pH 5.5 (squares), 6.5 (circles), 7.4 (triangles) and 8.5 (inverted triangles). Currents were normalized for individual oocytes to currents at  $+100$  mV in ND96 (pH 7.4). Mean currents at 60 mV were  $1.18 \pm 0.17 \mu A$  ( $\pm$ s.e.m.) for CIC-5 and  $1.07 \pm 0.36 \mu A$  ( $\pm$ s.e.m.) for CIC-5(E211A). Averages are from six oocytes (**a**) and ten oocytes (**b**) (two batches each). **c**, Extracellular pH dependence of currents at  $+100$  mV for CIC-5 (squares) and CIC-5(E211A) (circles). Currents were normalized to values at pH 7.4. Similar effects were seen for CIC-4(E224A) (data not shown). **d**, Intracellular pH of a tsA201 cell expressing CIC-5(E211A) is unaffected by depolarization (done as in Fig. 1a–c). Similar results were obtained in 11 and 4 experiments for CIC-5(E211A) and CIC-4(E224A), respectively.

$Cl^-/H^+$  coupling by comparing the rate of alkalinization to currents measured in experiments such as the one shown in Fig. 1b. For individual cells expressing either CIC-4 or CIC-5, their intracellular pH change ( $\Delta pH_i/\Delta t$ ) was used to estimate  $H^+$  fluxes. The calculation was based on the published buffer capacity of HEK cells<sup>12</sup> and on estimates of cell volume obtained from the area occupied by the individual cell (see Methods). These  $H^+$  fluxes were related to clamp currents to yield estimates for the coupling stoichiometry for an exchange of  $nCl^-$  for  $1H^+$ . Values thus obtained for individual cells were averaged. Under these assumptions,  $n$  was calculated as  $1.6 \pm 0.7$  (s.d., 6 cells) for CIC-4 and  $n = 1.5 \pm 0.7$  (11 cells) for CIC-5. However, uncertainties in buffer capacity<sup>12,13</sup>, cell volume and possible contributions of leak currents and  $H^+$  transport over the perforated patch<sup>14</sup> only allow us to give a rough estimate of  $1 \leq n \leq 5$ . This estimate agrees well with the approximate stoichiometry of 2 for CIC-e1, as determined with the easier and more exact determination of reversal potentials<sup>8</sup>.  $H^+$  and  $Cl^-$  transport mediated by CIC-4 and CIC-5 have the same order of magnitude, suggesting that  $H^+$  transport by endosomal CLCs might have a functional impact.

In the bacterial protein, flux coupling required the presence of a glutamate in the extracellular access pathway to the pore<sup>8</sup>. Similarly, fluxes of CIC-4 and CIC-5 were not just uncoupled in the absence of this glutamate, but also, similar to CIC-e1, both mammalian proteins displayed a low or negligible permeability to  $H^+$ . Experiments such as the one shown in Fig. 2d impose an upper limit on the  $H^+$  permeability of the glutamate mutant ( $<1/20$  of the  $Cl^-$  permeability). It appears to behave like a pure  $Cl^-$  conductance. Because current magnitudes were not significantly increased by this mutation (Fig. 2) (with comparable protein levels; data not shown), the

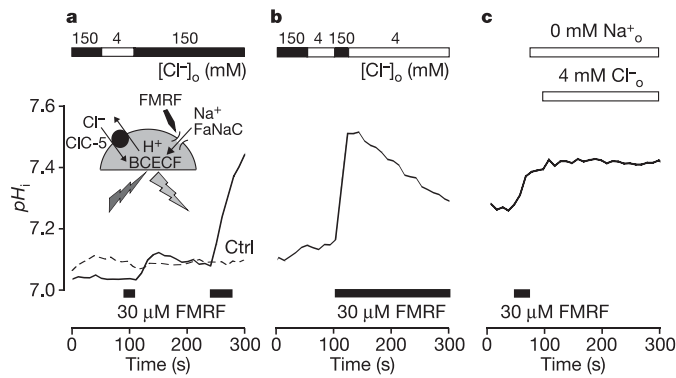


**Figure 3** |  $H^+$  transport depends on chloride and voltage. **a**, tsA201 cells transfected with CIC-5 and the ligand-gated  $Na^+$  channel FaNaC<sup>10</sup> were loaded with the pH indicator BCECF (inset). FMRFamide depolarized such cells to  $28 \pm 4$  mV ( $n = 8$ ) in Ringer's solution (data not shown) and changed intracellular pH with 150 mM, but not with 4 mM,  $Cl^-$ . FaNaC remained partially activated when removing FMRFamide, resulting in a moderate alkalinization with 150 mM  $Cl^-$ . Intracellular pH was unchanged in a non-transfected cell (dashed line; Ctrl) on the same coverslip. **b**, The alkalinization after depolarizing a cell expressing CIC-5 and FaNaC with FMRFamide in the presence of 150 mM  $Cl^-$  is reversed when changing to 4 mM  $Cl^-$  in the continued presence of FMRFamide. A similar acidification upon low  $[Cl^-]_o$  was seen in 11 cells. **c**, A cell expressing CIC-4 and FaNaC was alkalinized by applying FMRFamide. Subsequent  $Na^+$  removal should inhibit CIC-4 by hyperpolarization. Lowering  $[Cl^-]_o$  to 4 mM failed to change intracellular pH. Similar results were obtained with eight cells.

respective transport mechanisms probably do not differ as fundamentally as generally assumed when transporters are distinguished from channels. Notably, mutation of the glutamate changed the voltage dependence of CIC-3, CIC-4 and CIC-5 from strongly rectifying to linear<sup>7,15</sup>. Similar changes in voltage dependence were found for CIC-0 (refs 16, 17) and CIC-K<sup>18</sup> channels, where they were attributed to effects on the gating of a diffusion pore<sup>1,16</sup>. It is intriguing that the same residue is crucial for coupling  $Cl^-$  to  $H^+$  fluxes in CIC-e1, CIC-4 and CIC-5, for the voltage dependence of ion exchange in CIC-3, CIC-4 and CIC-5, and for voltage-dependent gating in CIC-0 (refs 16, 17) and CIC-1 (ref. 19).

Vesicular CLCs are thought to electrically compensate currents of  $H^+$ -ATPases in endosomal/lysosomal compartments, thereby facilitating their acidification<sup>2,4,15,20–23</sup>. Indeed, the acidification of endosomes and synaptic vesicles was impaired when CIC-5 or CIC-3 were disrupted<sup>2,20–24</sup>. The highly electrogenic  $Cl^-/H^+$  exchange of CIC-4 and CIC-5 remains compatible with this concept, but the coupling to an  $H^+$  counterflux implies that more metabolic energy is needed for acidification. Unlike  $Cl^-$  channels,  $Cl^-/H^+$  exchangers will directly couple  $Cl^-$  gradients to vesicular pH gradients. The vesicular  $Cl^-$  concentration might influence enzymatic activities<sup>25</sup> or might impinge on the osmotic regulation of vesicular volume. Additionally, CIC-4 and CIC-5 might directly acidify endosomes shortly after they pinch off from the plasma membrane by exchanging cytosolic  $H^+$  for luminal  $Cl^-$ , which initially is present at the high extracellular concentration. As discussed previously<sup>1,26</sup>, the role of the steep voltage dependence of CIC-4 and CIC-5 is enigmatic. Our work demonstrates that  $Cl^-/H^+$  exchange activity is not just a peculiarity of a bacterial CLC protein<sup>8</sup>, but rather that a dichotomy between transporters and channels exists within the mammalian CLC family. It additionally suggests a physiological role for vesicular CLCs not only in facilitating endosomal acidification, but also in regulating the  $Cl^-$  concentration in endosomal compartments.

## METHODS

**Perforated patch-clamp and intracellular pH measurements.** tsA201 cells (a large T-antigen-expressing derivative of HEK cells) were co-transfected with CLC complementary DNAs (CIC-0, CIC-4, CIC-5, CIC-4 (E224A) and CIC-5 (E211A))

cloned into pCIneo or pCDNA3 expression vectors, and a CD8-encoding plasmid as transfection marker, using Fugene (Roche). Before inserting a dish to the stage of an Olympus BX50WI upright microscope equipped with a  $\times 40$  lens, Imago CCD camera and Polychrome IV illumination system (T.I.L.L.), cells were loaded for 15–30 min with BCECF-AM ( $1 \mu\text{g ml}^{-1}$ ; Molecular Probes) in Ringer's solution (145 mM NaCl, 5 mM KCl, 5 mM glucose, 1 mM  $MgCl_2$ , 1.3 mM Ca-gluconate, 5 mM HEPES, pH 7.4) supplemented with anti-CD8-coated beads (Dynal) at room temperature. Cells were patched in Ringer's solution. When buffered to pH 5 (Fig. 1c), MES replaced HEPES. Patch pipettes connected to the head stage of an Axopatch 200A contained (in mM): 150 KCl, 1  $MgCl_2$ , 1.3  $CaCl_2$ , 5 HEPES, pH 7.4 and  $100 \mu\text{g ml}^{-1}$  gramicidin (Sigma). After gigaseal formation on CD8-positive cells and when gramicidin had lowered the access resistance to  $<100$ – $200$  M $\Omega$ , the clamp protocol and fluorescence acquisition were started. Owing to the access resistance, the voltages indicated in the corresponding figures are upper estimates of membrane voltages. BCECF was excited at 440 and 480 nm and the ratio of emission at  $\sim 520$  nm was converted to pH after calibration using nigericin and valinomycin ( $10 \mu\text{M}$  each) in KCl-based solutions buffered to pH values between 6.5 and 9. Data were analysed using T.I.L.L. Vision, pClamp9 and Origin7.

**Intracellular pH measurements on cells depolarized by FaNaC.** tsA201 cells were transiently co-transfected with CIC-5 (wild type or E211A mutant)<sup>7</sup> in pCDNA3 and FaNaC<sup>10</sup> in a bicistronic pIRES vector that co-expresses CD8 (ref. 11). Cells were seeded 24–36 h after transfection on laminin-coated coverslips and measured after 3 h. Cells were loaded with BCECF-AM for ratiometric fluorescence microscopy using an inverted microscope (Zeiss Axiovert 100) with a  $\times 100$  oil immersion lens. Fluorescence images were acquired with a CCD camera (Hamamatsu C4742-95) using excitation at 440 nm and 480 nm (Polychrome II, T.I.L.L.). Image acquisition and analysis used Openlab4 (Improvision). FaNaC-transfected cells were identified as above. Cells were continuously perfused with Ringer's solution.  $Cl^-$  was replaced by gluconate<sup>-</sup>;  $Na^+$  by NMDG<sup>+</sup> or by isomolar sucrose when replacing NaCl. FMRFamide was from Bachem. Fluorescence ratios were converted to pH as described above.

**Estimation of stoichiometry of  $Cl^-$  to  $H^+$  coupling.**  $H^+$  fluxes were estimated from cells transfected with CIC-4 or CIC-5 that were clamped to 60 mV as in Fig. 1.  $\Delta pH_i/\Delta t$  was converted to the  $H^+$  flux  $j(H^+)$  ( $\text{mol s}^{-1}$ ) taking the published value of the buffer capacity ( $\beta = 47 \pm 2$  mM  $H^+$  per pH unit) of parent HEK cells<sup>12</sup> and estimating the volume of the patched cell from its individual area  $A$ , as measured during ion imaging (mean  $431 \pm 28 \mu\text{m}^2$ ), multiplied by the mean height  $\bar{h}$  of tsA201 cells ( $10.1 \pm 1.0 \mu\text{m}$ ) measured by confocal stacks according to:

$$j(H^+) = \beta \frac{\Delta pH_i}{\Delta t} A \bar{h}$$

$Cl^-$  fluxes were calculated as  $j(Cl^-) = I/F - j(H^+)$ , where  $I$  is the clamp current and  $F$  is Faraday's constant. The apparent coupling ratio  $n = j(Cl^-)/j(H^+)$  was then calculated individually for each cell and averaged.

**Expression in *Xenopus* oocytes.** Capped cRNA was transcribed from CLC constructs cloned in pTLN. Oocytes were prepared, injected and measured as described<sup>7</sup>. Standard extracellular saline was ND96 (105 mM  $Cl^-$ , pH 7.4). pH was buffered with HEPES, MES and Tris as appropriate.

Received 11 February; accepted 25 May 2005.

- Jentsch, T. J., Poët, M., Fuhrmann, J. C. & Zdebik, A. A. Physiological functions of CLC  $Cl^-$  channels gleaned from human genetic disease and mouse models. *Annu. Rev. Physiol.* **67**, 779–807 (2005).
- Piwon, N., Günther, W., Schwake, M., Bösl, M. R. & Jentsch, T. J. CIC-5  $Cl^-$ -channel disruption impairs endocytosis in a mouse model for Dent's disease. *Nature* **408**, 369–373 (2000).
- Lloyd, S. E. *et al.* A common molecular basis for three inherited kidney stone diseases. *Nature* **379**, 445–449 (1996).
- Kornak, U. *et al.* Loss of the CIC-7 chloride channel leads to osteopetrosis in mice and man. *Cell* **104**, 205–215 (2001).
- Kasper, D. *et al.* Loss of the chloride channel CIC-7 leads to lysosomal storage disease and neurodegeneration. *EMBO J.* **24**, 1079–1091 (2005).
- Steinmeyer, K., Schwappach, B., Bens, M., Vandewalle, A. & Jentsch, T. J. Cloning and functional expression of rat CIC-5, a chloride channel related to kidney disease. *J. Biol. Chem.* **270**, 31172–31177 (1995).
- Friedrich, T., Breiderhoff, T. & Jentsch, T. J. Mutational analysis demonstrates that CIC-4 and CIC-5 directly mediate plasma membrane currents. *J. Biol. Chem.* **274**, 896–902 (1999).
- Accardi, A. & Miller, C. Secondary active transport mediated by a prokaryotic homologue of CLC  $Cl^-$  channels. *Nature* **427**, 803–807 (2004).
- Dutzler, R., Campbell, E. B., Cadene, M., Chait, B. T. & MacKinnon, R. X-ray structure of a CLC chloride channel at 3.0 Å reveals the molecular basis of anion selectivity. *Nature* **415**, 287–294 (2002).
- Lingueglia, E., Champigny, G., Lazdunski, M. & Barbry, P. Cloning of the

- amiloride-sensitive FMRamide peptide-gated sodium channel. *Nature* **378**, 730–733 (1995).
11. Poët, M. *et al.* Exploration of the pore structure of a peptide-gated Na<sup>+</sup> channel. *EMBO J.* **20**, 5595–5602 (2001).
  12. Soleimani, M. *et al.* Pendrin: an apical Cl<sup>-</sup>/OH<sup>-</sup>/HCO<sub>3</sub><sup>-</sup> exchanger in the kidney cortex. *Am. J. Physiol. Renal Physiol.* **280**, F356–F364 (2001).
  13. Roos, A. & Boron, W. F. Intracellular pH. *Physiol. Rev.* **61**, 296–434 (1981).
  14. Myers, V. B. & Haydon, D. A. Ion transfer across lipid membranes in the presence of gramicidin A. II. The ion selectivity. *Biochim. Biophys. Acta* **274**, 313–322 (1972).
  15. Li, X., Wang, T., Zhao, Z. & Weinman, S. A. The CIC-3 chloride channel promotes acidification of lysosomes in CHO-K1 and Huh-7 cells. *Am. J. Physiol. Cell Physiol.* **282**, C1483–C1491 (2002).
  16. Dutzler, R., Campbell, E. B. & MacKinnon, R. Gating the selectivity filter in CIC chloride channels. *Science* **300**, 108–112 (2003).
  17. Traverso, S., Elia, L. & Pusch, M. Gating competence of constitutively open CLC-0 mutants revealed by the interaction with a small organic inhibitor. *J. Gen. Physiol.* **122**, 295–306 (2003).
  18. Waldegger, S. & Jentsch, T. J. Functional and structural analysis of CIC-K chloride channels involved in renal disease. *J. Biol. Chem.* **275**, 24527–24533 (2000).
  19. Fahlke, C., Yu, H. T., Beck, C. L., Rhodes, T. H. & George, A. L. Jr Pore-forming segments in voltage-gated chloride channels. *Nature* **390**, 529–532 (1997).
  20. Günther, W., Piwon, N. & Jentsch, T. J. The CIC-5 chloride channel knock-out mouse — an animal model for Dent's disease. *Pflügers Arch.* **445**, 456–462 (2003).
  21. Stobrawa, S. M. *et al.* Disruption of CIC-3, a chloride channel expressed on synaptic vesicles, leads to a loss of the hippocampus. *Neuron* **29**, 185–196 (2001).
  22. Hara-Chikuma, M. *et al.* CIC-3 chloride channels facilitate endosomal acidification and chloride accumulation. *J. Biol. Chem.* **280**, 1241–1247 (2005).
  23. Yoshikawa, M. *et al.* CLC-3 deficiency leads to phenotypes similar to human neuronal ceroid lipofuscinosis. *Genes Cells* **7**, 597–605 (2002).
  24. Hara-Chikuma, M., Wang, Y., Guggino, S. E., Guggino, W. B. & Verkman, A. S. Impaired acidification in early endosomes of CIC-5 deficient proximal tubule. *Biochem. Biophys. Res. Commun.* **329**, 941–946 (2005).
  25. Davis-Kaplan, S. R., Askwith, C. C., Bengtzen, A. C., Radisky, D. & Kaplan, J. Chloride is an allosteric effector of copper assembly for the yeast multicopper oxidase Fet3p: an unexpected role for intracellular chloride channels. *Proc. Natl Acad. Sci. USA* **95**, 13641–13645 (1998).
  26. Jentsch, T. J., Stein, V., Weinreich, F. & Zdebik, A. A. Molecular structure and physiological function of chloride channels. *Physiol. Rev.* **82**, 503–568 (2002).

**Acknowledgements** We thank M. Lazdunski for the gift of the FaNaC-CD8 expression vector, and M. Petersen and P. Breiden for technical assistance. This work was supported in part by the Prix Louis-Jeantet de Médecine.

**Author Information** Reprints and permissions information is available at [npg.nature.com/reprintsandpermissions](http://npg.nature.com/reprintsandpermissions). The authors declare no competing financial interests. Correspondence and requests for materials should be addressed to T.J.J. (Jentsch@zmn.uni-hamburg.de).